Supporting Information

Wagatsuma et al. 10.1073/pnas.1714082115

SI Materials and Methods

Animals. All experiments used male mice between 12 and 25 wk old. The breeding room is maintained on a 12:12 light/dark schedule, and all experiments were carried out during the light cycle, except for calcium-imaging experiments, which were carried out during the dark cycle. All procedures were performed in accordance with US NIH guidelines, the MIT Department of Comparative Medicine and Committee on Animal Care. We created NET-Cre transgenic mice on a C57BL/6J background (Jackson Laboratory). The BAC clone RP23-326N7 (200 kb), including the *Slc6a2* (NET) promoter and gene, was transferred to the EL250 bacterial strain. The Cre sequence was inserted in-frame into the first exon shared by the major *Slc6a2* isoforms. The BAC-modifying cassette consisted of a 5′ homology arm, the Cre coding region in frame with the *Slc6a2* first exon sequence, the kanamycin-resistant gene flanked by FRTs (FLP recombinase targets), and a 3′ homology arm. The purified BAC-modifying cassette was electroporated into EL250 cells containing the RP23-326N7 BAC and was screened by PCR and Southern hybridization. For studies of optogenetic inhibition, we used the Cre/*lox*P recombinase system in transgenic animals to express Arch-EGFP in LC cells. The transgenic mouse Cre-responder line contains a *lox*P-flanked STOP cassette upstream of the Arch-EGFP fusion gene at the Rosa 26 locus in the cassette: Rosa-CAG-LSL-Arch-EGFP-WPRE-pA strain B6 (19) (stock no. 012735; The Jackson Laboratory). These Cre-responder mice were crossed with NET-Cre mice to obtain Arch/NET mice that express Arch-EGFP in the LC neurons. For studies of activity-dependent cell labeling, we crossed c-fos:tTA transgenic mice with NET-Cre mice. For studies of calcium imaging, we crossed KA1-Cre mice, in which Cre recombinase expression is robust in the CA3 pyramidal cell layer (21), with NET-Cre mice.

Stereotaxic Surgeries. All mice were single housed after surgery and had continuous access to food and water. Stereotactic viral injections, optic fiber implantations, microendoscope implantations, and microinfusion cannulae implantations were performed in accordance with the guidelines of the MIT Department of Comparative Medicine and Committee on Animal Care. Mice were anesthetized using 500 mg/kg tribromoethanol. Viruses and CTB488 were injected using a glass micropipette attached to a 10-μL Hamilton microsyringe through a microelectrode holder filled with mineral oil. A microsyringe pump and its controller were used to control the speed of the injection. Adeno-associated virus (AAV) and CTB injections were aimed at the following coordinates relative to bregma: anteroposterior (AP): −5.50 mm, mediolateral (ML): ±0.9 mm, dorsoventral (DV): −3.6 mm for the LC; AP: −2.05 mm, ML: ±2.1 mm, DV: −2.0 mm for CA3; AP: −2.0 mm, ML: ±1.0 mm, DV: −1.5 mm for CA1; and AP: −1.8 mm, ML: ±1.0 mm, DV: −2.1 mm for the DG. Optic fiber and microinfusion implantations were aimed at the following coordinates: AP: −5.5 mm, ML: ±0.9 mm, DV: −3.5 mm for the LC; AP: −2.05 mm, ML: ±2.1 mm, DV: −1.0 mm for CA3; and AP: −1.8 mm, ML: ±1.2 mm, DV: −1.9 mm for the DG. For GCaMP6f monitoring, unilateral viral delivery into the right CA3 was aimed at the following coordinates: AP: −1.7 mm, ML: ±2.0 mm, DV: −2.15 mm for CA3. Four weeks after AAV injection, a microendoscope was placed just above laterodorsal CA3 to minimize the damage of the hippocampal formation. All animals were allowed to recover and express sufficient opsin amounts for at least 4 wk before recording.

Immunohistochemistry. Mice were transcardially perfused with 4% paraformaldehyde (PFA) in PBS. Brains were postfixed with 4% PFA for 24 h and then cryoprotected in 30% sucrose in PBS for 24 h. Tissues were embedded in mounting medium, frozen, and then sectioned using a cryostat. For immunohistochemistry, sliced tissue sections were incubated with 0.5% Triton-X and 5% normal goat serum in PBS for 30 min, then in primary antibodies against GFP (A10262; 1:1,000; Invitrogen), RGS14 (75-170; 1:200; NeuroMab), TH (MAB318; 1:1,000; Millipore), NET (AB_2571810; 1:1,000; Frontier Institute), and c-Fos (SC-52; 1:500; Santa Cruz). After washing in PBS, sections were incubated in secondary antibodies conjugated with Alexa Fluor-488, -555, or -633 (1:400; Invitrogen). Before mounting, slices were incubated with DAPI (1 μg/mL) for 20 min. Images were taken using a confocal microscope (Leica).

Drug Delivery. For the novel context recognition test, we stereotaxically implanted guide cannulae targeting CA3 bilaterally. Animals were allowed to recover at least 2 wk before behavioral assessment. We infused 1 nL of 5 μg SCH23390, 10 μg propranolol, or saline via the guide cannulae bilaterally, 20 min before testing. For the calcium imaging experiment, 5 mL/kg CNO or saline was delivered i.p. 30 min before recording. All behavioral subjects were individually habituated to handling by the investigator at least for 3 d.

Behavior.

Novel-context recognition test in the open field. Behavioral recording and tracking were performed by EthoVision XT software (Noldus), using an IR-sensitive gigabit Ethernet (GigE) camera (Noldus) with two IR illuminators (XIRL-AT8S; Noldus) under dim dark conditions. During the sampling session, mice were exposed for 4 min to an open-field chamber that they had never experienced previously. Then, during the test session 24 h after the sampling session, mice were reexposed to the same chamber with the cues unchanged. Due to their preference for novelty, when mice recognize the test chamber as familiar, they explore the chamber less than they did on the sampling day (Fig. S2*A*) (20).

CFC. Behavioral recording and tracking were performed by FreezeFrame Software (ActiMetrics), using a digital video camera under dim conditions. The conditioning chambers A and B were rectangular in shape (29 cm long × 23 cm wide × 20 cm high), and their walls were made of clear Plexiglas. The two chambers had distinct visual cues, floor materials, odors, and top inserts. The two contexts were counterbalanced. The mouse was placed in a conditioning chamber and allowed to explore for 180 s, at which point a 2-s 0.75-mA foot-shock was delivered. The mouse remained in the conditioning chamber for a total of 210 s. On day 2 (24 h later), the mouse was placed into the conditioned chamber and allowed to explore for 300 s to recall contextual fear memory. On day 3, the mouse was placed into the distinct unconditioned chamber and allowed to explore for 300 s. Between tests, the test chamber was thoroughly cleaned with 75% ethanol or Quatricide (Pharmacal Research Labs).

CFC with preexposure. There is ample literature indicating that preexposure can impair subsequent associative learning under some conditions (latent inhibition) (42). To avoid this possibility, we used an established behavioral procedure with a short (10-s) duration of recall; previous studies have confirmed that use of this protocol results in successful conditioning of the context in rodents (7, 43, 44). The mouse was preexposed to a conditioning chamber and allowed to explore for 10 min on day 1. On the following day,

the animal was returned to the conditioned chamber for an 8-s exposure followed by a 0.75-mA foot shock and was removed from the chamber immediately. On day 3, the mouse was placed into the conditioned chamber and allowed to explore for 300 s to recall contextual fear memory. On day 4, the mouse was placed into the distinct unconditioned chamber and allowed to explore for 300 s. Mice are unable to acquire a full contextual representation rapidly in the fear-conditioning chamber (IS, 8-s exposure to context before shock delivery) but are able to associate context with shock if they are previously exposed to the context.

Cell Counting. The numbers of H2B-EGFP and c-Fos immunoreactive neurons in hippocampal subregions (two to four coronal slices per mouse) were counted to measure the number of cells active during novel and familiar environment exposure. Fluorescence images were acquired using a confocal microscope (Leica) with a 2×0/0.50 NA objective. All animals were killed 90 min postexposure on day 2. The number of $EGFP^+$ or c-Fos^+ cells in a set region (0.5 mm^2 per brain area analyzed) were quantified with ImageJ and averaged within each animal. Background noise was removed by applying a threshold "remove outlier" (radius, 2.0; threshold, 50; dark outlier). Boundaries of hippocampal subregions were manually identified by expression of RGS14, which is robust in CA2. Regions of interest (ROIs) were identified by "analyzed particles" (size, 150–1,000 pixels; circularity, 0.3–1.0), and fluorescence intensities of c-Fos images in each ROI were measured as absolute fluorescence magnitude. To calculate a random shuffling score for each sample (random fluorescence score), average fluorescence intensities of c-Fos images from a different mouse were used. The absolute fluorescence scores minus the random fluorescence score provided the normalized c-Fos fluorescence intensity.

In Vivo Calcium Imaging. After a mouse recovered from intracranial implantation of the microendoscope, the baseplate for a miniaturized microscope camera was attached above the microendoscope. After the baseplate surgery, the mouse was habituated to the attachment of the microscope camera, human handling, and needle penetration for 2 wk. Calcium imaging was performed during the dark cycle. The open-field chamber was rectangular (50 × 50 × 25 cm) (Fig. S2*C*), and its walls were made of clear Plexiglas. The context of the chamber could be changed in four ways: (*i*) the plastic white floor could be exchanged to a metal grid floor; (*ii*) clear walls could be covered by black inserts; (*iii*) 75% ethanol, 0.1% acetic acid, or 25% benzoaldehyde was added as an odor cue; and (*iv*) lighting of the experimental room could be varied with red lamps from darkness to dim lighting. Ca^{2+} imaging in the open field lasted 30 min to collect a sufficient number of Ca^{2+} transients for the statistical analyses. Two contexts were counterbalanced. Between tests, the test chamber was thoroughly cleaned with 75% ethanol or Quatricide.

As previously described (32), Ca^{2+} events were captured at 20 Hz on a miniature microscope (Inscopix). The calcium movie was then motion corrected using Mosaic software (Inscopix) [correction type: translation and rotation; reference region with spatial mean (r = 20 pixels) subtracted, inverted, and spatial mean applied (r = 5 pixels)]. Finally, it was processed by ImageJ [dividing each image, pixel by pixel, by a low-passed (r = 20 pixels) filtered version], and the ΔF/F signal was calculated.

Four hundred cell locations were selected from the resulting movie by principal component analysis-independent component analysis (PCA-ICA) [600 output principal components (PCs), 400 independent components (ICs), 0.1 weight of temporal information in spatiotemporal ICA, 750 iterations maximum, 1E-5 fractional change to end iterations] in Mosaic software, and the ICs were binarized with a threshold equal to half of the maximum intensity. ROIs that were not circular (length >2× width) were discarded. The temporal traces of the remaining ICs were collected. Calcium traces were calculated at these ICs for each processed movie. Calcium events were detected by thresholding (>2 SDs from the ΔF/F signal,) at the local maxima of the ΔF/F signal. Calcium events that occurred within 250 ms of a previous calcium event were excluded.

Behavioral recording and tracking were performed by EthoVision XT software (Noldus), using an IR-sensitive GigE camera (Noldus) with two IR illuminators (XIRL-AT8S; Noldus). The tracked positions were sorted into 5 × 5 cm spatial bins. The calcium event rate of each neuron was determined for each bin, and a rate map composed of all the spatial bins was produced. The rate map was smoothed with each pixel (spatial bin) boxcar averaged over the surrounding 5 × 5 pixels with a Gaussian smoothing kernel; σ = 2 pixels. The bins that had a calcium event rate less than 0.2 Hz were considered unreliable and were discarded from further analysis (set to zero). The rate maps for each individual neuron across two run sessions were treated as two vectors (lists of numbers), and a "similarity score," defined as Pearson's correlation coefficients between these two vectors, was calculated.

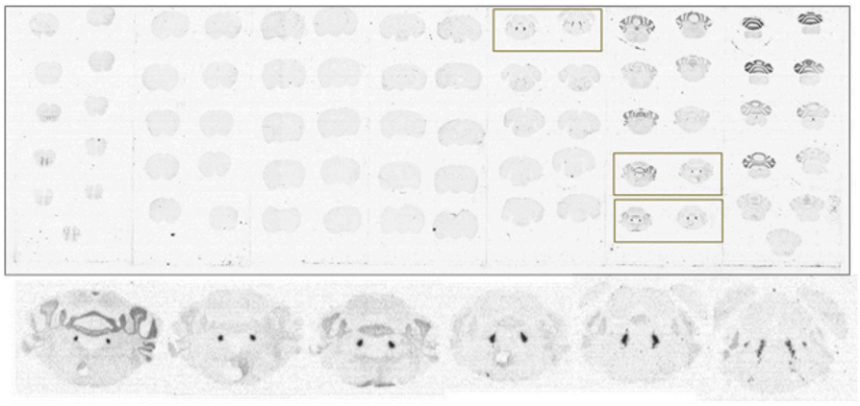

Fig. S1. *Cre* expression is robust in the LC of NET-Cre mice. In situ hybridization of an NET-Cre mouse shows the robust expression of *Cre* mRNA in the LC but not other brain regions.

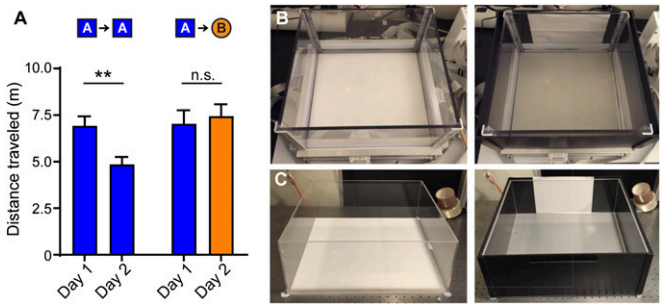

Fig. S2. The novel-context recognition test in wild-type mice. (*A*) Mice were exposed to novel context A on day 1 and were allowed to explore the context for 10 min. Mice were subsequently exposed to the same context A on days 2–4. When mice were exposed to another novel context, B, the exploration level of the context increased to the level of day 1. Statistical comparisons were performed using two-way repeated-measures ANOVA ($F_{1,20} = 10.41$, $P < 0.005$; $n = 11$ each) and post hoc Sidak's multiple comparisons test (**$P < 0.01$; n.s., not significant). Data are presented as mean ± SEM. (*B*) Open-field chambers A and B used for the novel-context recognition test. Wall color, odor, lighting, and floor material are different. Context A and B were counterbalanced. (*C*) Open-field chambers A and B used for in vivo Ca^{2+} imaging.

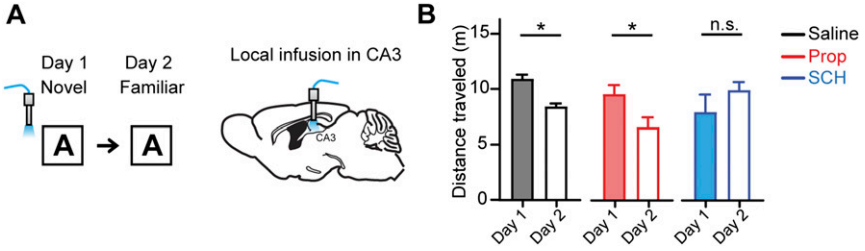

Fig. S3. Novel contextual memory is impaired by a drug targeting D1-like receptors in hippocampal CA3. (*A*) Drugs were infused 20 min before novel-context sessions. A microinfusion cannula was implanted above CA3. (*B*) The D1/D5 receptor antagonist SCH23390 (SCH) blocked novel contextual memory, whereas the β-adrenoreceptor antagonist propranolol (Prop) or saline had no effect. Statistical comparisons were performed using two-way repeated-measures ANOVA ($F_{2,24} = 7.508$, $P < 0.005$; $n = 9$ each group) with post hoc Sidak's multiple comparisons test (*$P < 0.05$; n.s., not significant). Data are presented as mean ± SEM.

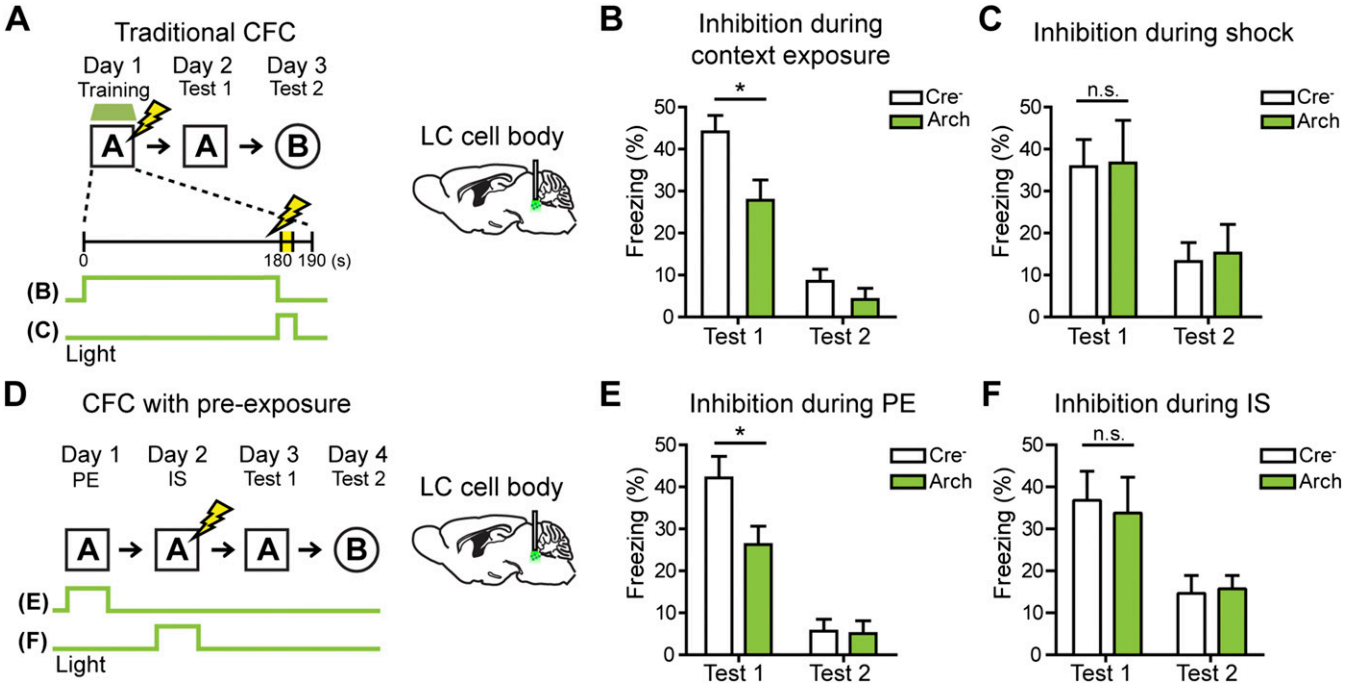

Fig. S4. Inhibition of LC cell body in CFC. (*A*) The behavioral schedule for traditional CFC. Sessions are 24 h apart. Green bars represent the timing of light delivery. (*B* and *C*) Freezing levels were averaged over 5-min test sessions in the conditioned context A (test 1) and unconditioned context B (test 2). Optogenetic inhibition was delivered from the beginning of the context exposure to 1 s before the electric shock (Cre^-, $n = 10$; Arch, $n = 9$) (*B*) or for 5 s including 2 s of electric shock ($n = 7$ per group) (*C*). (*D*) Behavioral schedule for preexposure-dependent CFC. (*E* and *F*) Optogenetic inhibition was delivered throughout the preexposure (PE) session for 10 min (*E*) or the immediate shock (IS) session (*F*). Bars show freezing levels with optogenetic inhibition during preexposure ($n = 6$ per group) (*E*) and during immediate shock (Cre^-, $n = 12$; Arch, $n = 11$) (*F*). Statistical comparisons were performed using unpaired *t*-tests; *$P < 0.05$; n.s., not significant. Data are presented as mean ± SEM.

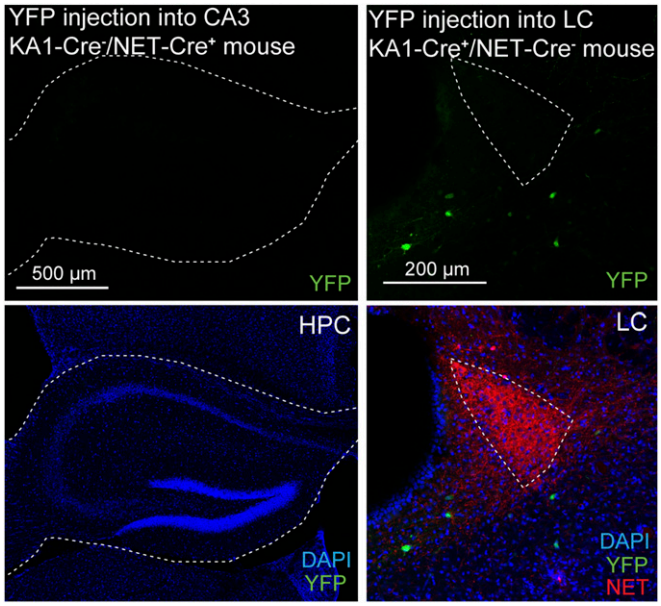

Fig. S5. Cre-dependent EYFP expression is limited in nontarget brain regions. (*Left*) Cre-dependent EYFP expression in a NET-Cre mouse. (*Right*) Cre-dependent EYFP expression in the LC of a KA1-Cre mouse. No YFP expression is observed in nontarget brain areas.

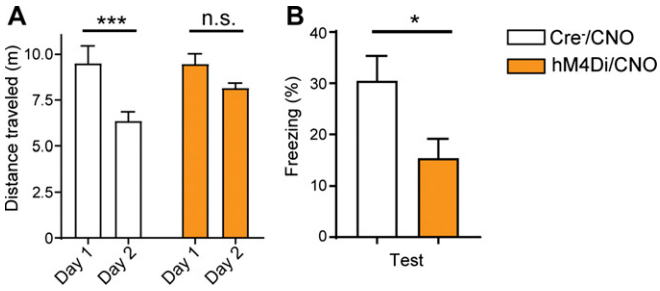

Fig. S6. Novel contextual memory is impaired when the LC is silenced using the inhibitory DREADDs system. AAV5-hsyn:DIO-hM4Di-mCherry was bilaterally injected into the LC of NET-Cre mice. CNO was i.p. injected 30 min before novel-context sessions. (*A*) Novel-context recognition test (two-way repeated-measures ANOVA; $F_{1,13} = 4.866$, $P < 0.05$; $n = 8$ for the Cre^- group and $n = 7$ for the hM4Di group; and post hoc Sidak's multiple comparisons test, $^{***}P < 0.005$; n.s., not significant). (*B*) Traditional CFC. Freezing levels were tested in the conditioned context 24 h after conditioning (unpaired *t* test; $^{*}P < 0.05$; $n = 6$ for the Cre^- group and $n = 5$ for the hM4Di group). Data are presented as mean ± SEM.